



Deposited via The University of Sheffield.

White Rose Research Online URL for this paper:

<https://eprints.whiterose.ac.uk/id/eprint/157261/>

Version: Accepted Version

Article:

Alshammari, A.H., Alqahtani, Z., Mohd Suah, F.B. et al. (2020) Low cost, high sensitivity detection of waterborne Al³⁺ cations and F⁻ anions via the fluorescence response of a morin derivative dye. *Analytica Chimica Acta*, 1105. pp. 1-10. ISSN: 0003-2670

<https://doi.org/10.1016/j.aca.2020.01.070>

Article available under the terms of the CC-BY-NC-ND licence
(<https://creativecommons.org/licenses/by-nc-nd/4.0/>).

Reuse

This article is distributed under the terms of the Creative Commons Attribution-NonCommercial-NoDerivs (CC BY-NC-ND) licence. This licence only allows you to download this work and share it with others as long as you credit the authors, but you can't change the article in any way or use it commercially. More information and the full terms of the licence here: <https://creativecommons.org/licenses/>

Takedown

If you consider content in White Rose Research Online to be in breach of UK law, please notify us by emailing eprints@whiterose.ac.uk including the URL of the record and the reason for the withdrawal request.

Low cost, high sensitivity detection of waterborne Al^{3+} cations and F^- anions via the fluorescence response of a morin derivative dye.

Alhulw H. Alshammari^{*1,2}, Zahrah Alqahtani^{1,3}, Faiz Bukhari Mohd Suah⁴, Syaza Atikah Nizar⁴, Alan Dunbar⁵, and Martin Grell¹

¹Physics and Astronomy, University of Sheffield, Hicks Building, Hounsfield Rd, Sheffield S3 7RH, UK

²College of Science, Aljouf University, Airport ST, Sakaka 72388, Saudi Arabia

³Department of Physics, University of Taif, Taif-Al-Haweiah 21974, Saudi Arabia

⁴School of Chemical Sciences, Universiti Sains Malaysia (USM), 11800 Minden, Pulau Pinang, Malaysia

⁵Chemical and Biological Engineering, The University of Sheffield, Mappin St, Sheffield S1 3JD, UK

*Corresponding author, Ahfalshammari1@sheffield.ac.uk

Abstract

Morin dye is known as a cheap and readily available selective 'off → on' fluorescent sensitiser when immobilised in a phase transfer membrane for the detection of Al^{3+} ions. Here, a morin derivative, NaMSA, which readily dissolves in water with good long-term stability is used in conjunction with a fibre optic transducer with lock-in detection to detect Al^{3+} in drinking water below the potability limit. The combination of a water soluble dye and the fibre optic transducer require neither membrane preparation nor a fluorescence spectrometer yet still display a high figure-of-merit. The known ability to recover morin-based Al^{3+} cation sensors selectively by exposure to fluoride (F^-) anions is further developed enabling a complementary sensing of either fluoride anions, or aluminium cations, using the same dye with a sub-micromolar limit-of-detection for both ions. The sensor performance parameters compare favourably to prior reports on both aqueous aluminium and fluoride ion sensing.

Keywords: Morin, Aluminium, Fluoride, Fibre Optics

1. Introduction

Aluminum is commonly used in food packing, clinical tools, food processing equipment, kettles and water pipes. Metallic aluminium is slightly soluble in aqueous media in the form of its Al^{3+} cation [1]. Intake of Al^{3+} into the human body may cause serious diseases, including Alzheimer's [2,3] and Parkinson's [3] diseases. The concentration of Al^{3+} in drinking water is therefore regulated to a 'potability limit' of $7.4 \mu\text{M}$ [4]. Consequently, a number of analytical techniques have been developed to quantify Al^{3+} in water, including spectrophotometric [5], fluorimetric [6,7], and electrochemical [8] sensors. An important Al^{3+} selective ionophore is 2',3,4',5,7-Pentahydroxyflavone, known as 'morin', is shown in Fig. 1a. Morin is known to selectively complex with waterborne Al^{3+} , forming a $[\text{morin}:\text{Al}^{3+}]$ complex. Morin has therefore been used both as an ionophore in electrochemical Al^{3+} sensors [8] and in 'off \rightarrow on' fluorescent sensors [9] because the $[\text{morin}:\text{Al}^{3+}]$ complex shows cyan- coloured fluorescence while uncomplexed morin does not show fluorescence [6]. The $[\text{morin}:\text{Al}^{3+}]$ complex which has poor solubility in buffered aqueous solution absorbs light between 400 nm to 440 nm and emits a broad band between 500 nm and 560 nm [10]. Embedding morin in a permeable membrane which allows the transfer of Al^{3+} enables it to be used as an Al^{3+} sensor [9]. Alternatively, Kopacz [11] has described a chemical modification of morin into a sodium salt of morin sulfonic acid, NaMSA, Fig. 1b, that dissolves well in water (dissociating into $\text{Na}^+ / \text{MSA}^-$), without the need to promote solubility by adding organic solvents as is required for some other ion- selective fluorophores, *e.g.* [12-15]. NaMSA can still be immobilised in a permeable membrane [6], but preparation of such membranes is difficult and time- consuming. Plasticised PVC membranes often show slow responses [16] and may suffer from dye leaching [17]. In this work, we take advantage of the good solubility of NaMSA in water to extend the use of NaMSA as an Al^{3+} - selective 'off \rightarrow on' fluorescent sensitiser [9,18] when immobilised in a phase transfer membrane to a morin derivative, instead using the NaMSA dissolved in water, avoiding the need for membrane preparation. We find that dissolved NaMSA retains its ability to complex with Al^{3+} into a fluorescent $[\text{MSA}^-:\text{Al}^{3+}]$ complex, fig. 1c. We quantify Al^{3+} in water samples by fluorimetry using dissolved NaMSA. Instead of a conventional

spectrofluorimeter, we adopted a fibre- optic fluorimeter with LED excitation and lock-in amplification which has been described previously [19] for solution- based fluorimetry. We establish a limit-of-detection (LoD) for Al^{3+} below the potability limit, a high figure-of-merit for the fibre-optic instrument, and quantify Al^{3+} in a few example samples using the standard addition method [20]. Further, we take advantage of the possibility to recover NaMSA-based Al^{3+} sensors after use by treatment with concentrated fluoride (F^-) solutions [18]. We develop this into a complementary 'on \rightarrow off' fluorescent sensor for fluoride by prior 'activation' of the dissolved NaMSA with Al^{3+} to form the fluorescent $[\text{MSA}^-:\text{Al}^{3+}]$ complex that we then titrate with aliquots of fluoride to gradually turn its fluorescence off. Fluoride is another interesting analyte because small doses of fluoride are beneficial to bones and teeth [21], but higher doses can be detrimental causing fluorosis and urolithiasis [22]. Fluoride in drinking water is therefore subject to a potability limit of 79 μM [4]. Again we demonstrate a LoD well below the legal potability limit. In summary, we show the 'complementary' fluorimetric detection of two relevant ions (Al^{3+} and F^-) in water below their respective potability limits, using the same dye for both, together with a low- footprint instrument.

2. Experimental

a.) Synthesis and materials

Morin was purchased from Sigma Aldrich and chemically modified into the water- soluble sodium salt of morin sulfonic acid (NaMSA) following the route reported by Kopacz [11]. From an initial 10g of morin we obtain yield of $\sim 7\text{g}$ of NaMSA. Fig. 1 shows the chemical structure of morin, NaMSA, and the complex that NaMSA forms with Al^{3+} .

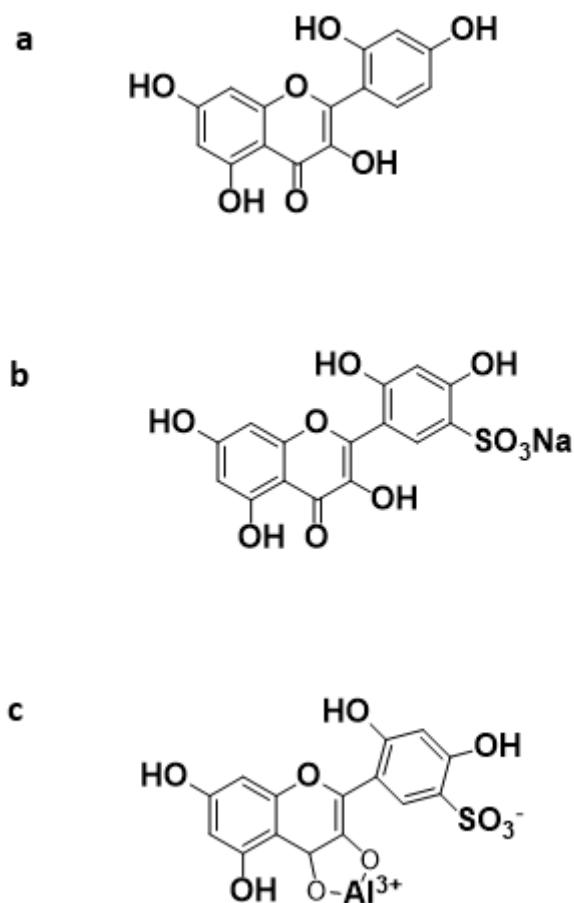


Fig.1. a.) Chemical structure of morin. b.) Structure of NaMSA. When dissolved in water, this dissociates into MSA^- and Na^+ . c.) Structure of $[\text{MSA}^-:\text{Al}^{3+}]$ complex that forms in aqueous solution when Al^{3+} is added to dissolved NaMSA.

Acetone, Hydrochloric acid 37% (HCL), aluminum nitrate nonahydrate $\text{Al}(\text{NO}_3)_3 \cdot 9\text{H}_2\text{O}$, sodium fluoride (NaF) and sodium chloride (NaCl) were obtained from Sigma aldrich.

b.) Overview of measurement setup

Fig. 2 gives an overview over our fibre optic lock-in fluorimeter. The instrument is adapted from earlier work [19,23].

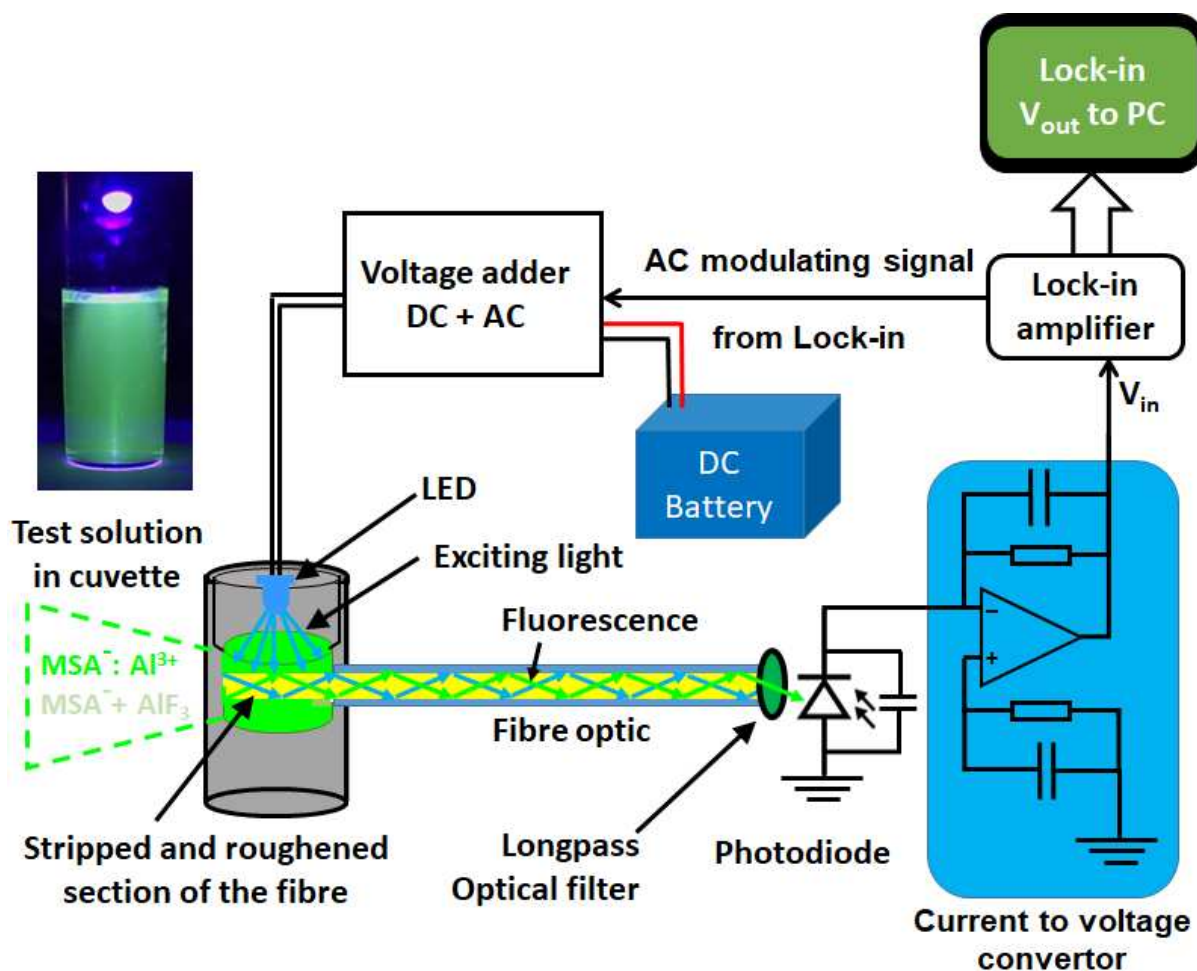


Fig. 2. Schematic diagram of our fibre- optic lock-in fluorimeter.

A mixture of the analyte sample and the fluorophore solution is held in a bespoke cuvette (Fig. 3) fitted with an optical fibre that has been treated to pick up fluorescence and guide it to a photodiode (PD) circuit for measurement. Fluorescence is excited using a 405 nm LED (LED 405 L, Thorlabs) at a distance of ~ 1.2 cm from the surface of the liquid in the cuvette at approximately a right angle. The LED is driven by the sum of a 5641 Hz AC voltage, amplitude 4.2 V, from a Lock In reference output plus a 8.15 V DC bias through a 150 Ω resistor. The optical power from the LED was measured using an optical power meter (PM100D, Thorlabs) at a distance of 1.2 cm and found to be 5.9 mW. This power when divided by the exposed surface area gives a power density of 83.1 W/m^2 .

A longpass optical filter with an edge at 488 nm (LP02-488RU-25, Semrock) is inserted before the PD to block the 405 nm excitation while allowing most of morin fluorescence to pass. The PD output current is fed into a current/voltage (I/V) converter with 100 k Ω feedback resistor, the I/V converter output then is AC coupled into the measurement input

of the same Anfatec digital lock-in that generated the reference signal, set to x100 analogue preamplification. The lock-in provides a DC output voltage, V_{out} , that is proportional to the AC component of the light intensity, F , picked up by the fibre. $V_{out}(t)$ is recorded over time by a bespoke LabView routine, an example is shown in Fig. 4.

c. Preparation of optical fibres

We used multimode optical fibres (FT1500UMT, Thorlabs) with a 1.5 mm silica core diameter and a 50 μm transparent polymer cladding, coated in a non-transparent outer 'buffer'. The refractive indices of the fibre's core and cladding are 1.467 and 1.406, respectively. 10 cm of fibre was cleaved from a reel and a 1 cm length of the fibre core was exposed at one end by stripping away both the cladding and the buffer. The fibre was then cleaned and dried as reported previously [23]. Since a smooth exposed fibre core picks up only very little fluorescence, the stripped section of the fibre was roughened all around its surface using a Dremel 'Corded Multi- Tool 3000' rotary tool as described previously [24].

d. Cuvettes

Bespoke cuvettes were manufactured by the University of Sheffield workshop, as shown in Fig. 3. Two cuvettes were made and while identical in shape, one was made of transparent PMMA as commonly used for conventional fluorimetric cuvettes, and the other was made of stainless steel. Cuvettes were polished on the inside so that the walls of the stainless steel cuvette act as a mirror to increase the amount of fluorescence picked up by the fibre.

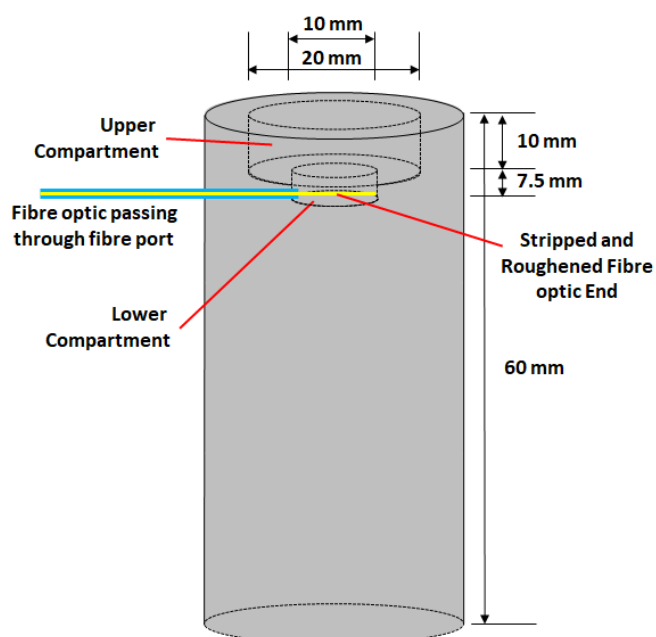


Fig. 3. Design of bespoke cuvettes, manufactured in our workshop. Cuvettes were made either of transparent material (PMMA), or a reflective material (stainless steel). The bottom compartment where the fibre is fitted has a capacity of 300 μL while a wider upper compartment holds liquid in excess of 300 μL .

e. Preparation of solutions

All solutions were prepared in deionised water of resistivity 15 $\text{M}\Omega\cdot\text{cm}$ at 20 $^{\circ}\text{C}$ as measured by our DI Water system that first had been acidified by adding hydrochloric acid (HCl) to adjust the pH to 5, as measured by a CyberScan pH meter 300. An acidic medium is required to prevent the formation of Al^{3+} hydroxide complexes [9] that would compete with $\text{MSA}^{-}/\text{Al}^{3+}$ complexation. Solutions of Al^{3+} (from Aluminium nitrate nonahydrate), F^{-} (from NaF), and Cl^{-} (from NaCl) for titration aliquots were prepared at a few concentrations (100 μM , 1 mM, 10 mM, 100 mM) by dissolving the required amount of their salts in 200 solution of the NaMSA fluorophore that were prepared in acidified water. For standard addition tests, three Al^{3+} solutions with concentrations in the order of the potability limit were prepared by a co-worker who was not otherwise involved with the work reported here. Concentrations were noted but not reported to the worker undertaking the standard addition test, but only labelled as 'A, B, C'. To prepare Al^{3+} sensitive solution, 200 μM solution of the NaMSA fluorophore is prepared in acidified water. A sample of the 200 μM fluorophore solution in acidified water was kept in the lab for two months to check the lifetime of the fluorophore. To 'activate' the NaMSA solution for fluoride sensing, we prepared a solution of $[\text{Al}^{3+}:\text{MSA}^{-}]$ complex by adding 15.8 μL of 1 mM Al^{3+} solution to 300 μL of 200 μM NaMSA solution, resulting in a ~ 50 μM solution of $[\text{Al}^{3+}:\text{MSA}^{-}]$ complex. We used an excess of dissolved NaMSA over Al^{3+} to make sure all the Al^{3+} ions complex with MSA^{-} , with no remaining free Al^{3+} . Again, some of the activated solution was kept in the lab for two months to check the lifetime of the solution. To test the effect of the simultaneous presence of fluoride and aluminium, a 1 mM solution of F^{-} (from NaF) and a 1 mM of Al^{3+} (from $\text{Al}(\text{NO}_3)_3$) were prepared in acidified NaMSA solution (pH = 5). Then these solutions were mixed in a 3:1 ratio of fluoride solution: aluminium solution by volume, resulting in a (0.75 mM F^{-} / 0.25 mM Al^{3+}) solution.

f. Titrations for sensor calibration

The Al^{3+} sensor was calibrated using 300 μL of NaMSA solution which was transferred into the PMMA or stainless steel cuvettes fitted with a roughened optical fibre, as described above. For titration, small amounts of Al^{3+} solutions that were dissolved in NaMSA solution were pipetted into the filled cuvettes and mixed by gentle stirring. Then the same volume as that just added was removed from the cuvette by pipette in order to keep the solution volume at exactly 300 μL , which is ~ 3 cm above the roughened fibre. This was done in order to ensure that the excitation geometry remained the same throughout the titration series. The new analyte concentration, c , was calculated from known volumes and concentrations of stock solutions. Pipetting was repeated to cover a range of concentrations from below μM to 10 mM. Fluorescence was excited continuously by the LED and the intensity was monitored over time via the lock-in amplifier output, V_{out} , and recorded by bespoke LabView routine. The F^- sensor was calibrated in a similar manner the Al^{3+} sensor calibration, only now we filled the cuvettes with $[\text{Al}^{3+}:\text{MSA}^-]$ complex solution instead of NaMSA solution. Then we added F^- aliquots to cover a range of concentrations from below μM to 6 mM. The fluorescence was excited and monitored exactly as in the Al^{3+} sensor calibration.

An example of the $V_{\text{out}}(t)$ trace resulting from a typical titration as described above is shown in Fig. 4.

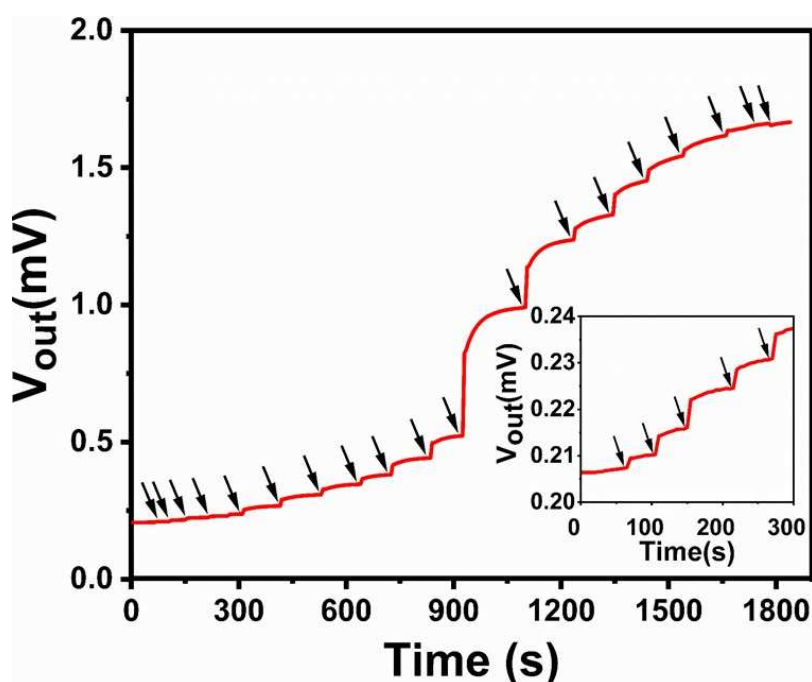


Fig. 4. Example of a V_{out} vs time series for NaMSA solution under stepwise additions of Al^{3+} aliquots. Every arrow indicates a titration step, *i.e.* addition of an Al^{3+} aliquot. Inset: Magnification of the short time / low Al^{3+} concentration region.

Although morin is an ‘off \rightarrow on’ dye, we note that even at $t = 0$, *i.e.* when the concentration $c = [\text{Al}^{3+}] = 0$, $V_{\text{out}}(0) > 0$. The initial $V_{\text{out}}(0)$ results from two contributions: namely, some of the exciting light still passes through the longpass optical filter between the fibre and the PD (no fluorescence involved), and uncomplexed MSA^- in solution is very weakly fluorescent (*i.e.* there is some fluorescence in the absence of analyte). We call the former ‘background’, and the latter ‘zero analyte fluorescence’. Taken together they give the initial $V_{\text{out}}(0)$. Note, ambient light does not contribute to $V_{\text{out}}(0)$ as the lock-in discards all signals at frequencies other than its reference frequency, making it ‘blind’ to ambient light.

For Al^{3+} standard addition titrations, the roughened fibre section was fitted into the PMMA cuvette, then 300 μL of 200 μM NaMSA was pipetted into the cuvette. The background $V_{\text{out}}(c = 0)$ was recorded, then the cuvette was washed three times with DI water, refilled with NaMSA solution and the background $V_{\text{out}}(c = 0)$ was recorded again; and this was repeated a few times. Results were very similar each time $V_{\text{out}} \sim 0.185 \text{ mV} \pm 0.02$ and were averaged to give an average background for later correction. The cuvette was again washed three times with DI water, then a 300 μL of solution of unknown concentration c_{sample} was pipetted into the cleaned cuvette, and $V_{\text{out}}(c = c_{\text{sample}})$ was recorded. Finally, solution of c_{sample} was titrated with aliquots of Al^{3+} solution of known concentration to increase c_{sample} by c_{added} in steps of 10 μM , and $V_{\text{out}}(c = c_{\text{sample}} + c_{\text{added}})$ was recorded after each titration.

g. Data analysis

The $V_{\text{out}}(t)$ data recorded during titrations as shown in Fig. 4 were converted into $V_{\text{out}}(c)$ by relating time to ion concentration, c . As a first step in the data analysis for ‘off \rightarrow on’ fluorescence, where we calibrated by adding increasing concentrations, c , of Al^{3+} to non-fluorescent NaMSA solution, we adjust all $V_{\text{out}}(c)$ data by subtracting the initial $V_{\text{out}}(0)$ prior to further analysis, hence $V_{\text{out}}(0) = 0$ by definition. On the other hand, for ‘on \rightarrow off’ fluorescence when we add aliquots of F^- to fluorescent $[\text{MSA}^-:\text{Al}^{3+}]$ complex, we adjust by subtracting the final $V_{\text{out}}(c \rightarrow \infty)$ from all data. Practically, $V_{\text{out}}(c \rightarrow \infty)$ was taken at a

concentration much larger than $c_{\frac{1}{2}} = 1/k$, see below. Hence, $V_{\text{out}}(c \rightarrow \infty)$ becomes 0 by definition. For further analysis of $V_{\text{out}}(c)$ which is proportional to $F(c)$, where $F(c)$ is the fluorescence intensity, we assume the fraction $\theta(c)$ of the dye complexed by the analyte at an analyte concentration c is given by a Langmuir-like relationship:

$$\text{eq. 1} \quad \theta(c) = \frac{kc}{(kc+1)}$$

With $0 \leq \theta(c) < 1$, and k is a stability constant. In colloquial terms, k quantifies the ‘strength’ of analyte / sensitizer interaction. More precisely, k is given by the enthalpy of complex formation, ΔH , via $k = \exp(-\Delta H / RT)$.

Properties of $\theta(c)$ are $\theta(0) = 0$, $\theta(c) \approx kc$ for $c \ll 1/k$, $\theta(c_{\frac{1}{2}}) = \frac{1}{2}$ for $c_{\frac{1}{2}} = 1/k$, and $\theta(c \rightarrow \infty) \rightarrow 1$. $V_{\text{out}}(c)$ will depend both on $\theta(c)$, and a number of parameters specific to a particular experimental setup (length and roughness of fibre, geometry and type of cuvette, intensity and alignment of excitation source, gain in the transimpedance amplifier, etc...) which will differ between different experimental runs. However, with the help of eq. 1 we can account for these parameters and determine the stability constant, k , and a limit-of-detection (LoD).

For ‘off \rightarrow on’ fluorescence, the dye in the absence of analyte is non-emissive (or weakly emissive but this is accounted by the aforementioned prior subtraction of $V_{\text{out}}(0)$), but becomes emissive in the presence of analyte. Here this was the case for sensing Al^{3+} with dissolved NaMSA. $V_{\text{out}}(c)$ is given by the relative fraction of complexed dye, $\theta(c)$:

$$\text{eq.2} \quad V_{\text{out}}(c) = V_{\infty} \theta(c) = V_{\infty} \frac{kc}{kc+1}$$

Wherein $V_{\infty} = V_{\text{out}}(c \rightarrow \infty)$. To determine k , we therefore fitted the experimental $V_{\text{out}}(c)$ data to eq. 2 using the non-linear fit routine in Origin 2018 software. To evaluate the limit-of-detection (LoD) for an ‘off \rightarrow on’ dye, we considered only the data for ‘small’ concentrations *i.e.* $c \ll 1/k$, where we expect a linear relationship, as $\theta(c) \approx kc$ for $c \ll 1/k$. For $c \ll 1/k$ we fitted with $V_{\text{out}}(c) = mc + b$ with slope m and intercept $b \pm \Delta b$, with b expected to overlap zero within at most $1.96 \Delta b$ (on a 5% significance level). The analyte concentration at the LoD, c_{LoD} , is then given by the common ‘3 errors’ criterion [25]:

$$\text{eq.3} \quad c_{\text{LoD}} = 3\Delta b/m$$

To determine unknown Al^{3+} concentrations we used the standard addition method [26]. We first subtract the previously established average background from all V_{out} data (cf. 2f), then plot background corrected $V_{\text{out}}(C_{\text{add}})$ vs C_{add} , fit a straight line and identify the previously unknown C_{sample} as the negative of the intercept of the fitted straight line with the (negative) C_{add} - axis.

For 'on \rightarrow off' fluorescence the dye in an analyte-free medium emits and adding analyte makes the dye become non-emissive. Here this was the case for the sensing of F^- with $[\text{Al}^{3+}:\text{MSA}^-]$ complex. Now, $V_{\text{out}}(c)$ is given by the fraction of remaining $[\text{Al}^{3+}:\text{MSA}^-]$ complex, $1 - \theta(c)$:

$$\text{eq.4} \quad V_{\text{out}}(c) = V_0 [1 - \theta(c)] = \frac{V_0}{(kc+1)}$$

Wherein $V_0 = V_{\text{out}}(c = 0)$. To determine k , we therefore fitted the experimental $V_{\text{out}}(c)$ data to eq. 4 using the non-linear fit routine in Origin 2018 software. To evaluate the LoD for an 'off \rightarrow on' dye we again consider only data at 'small' concentrations, $c \ll 1/k$, where eq. 4 can be approximated by eq. 5:

$$\text{eq. 5} \quad V_{\text{out}}(c) \approx V_0 (1 - kc) \Rightarrow 1 - V_{\text{out}}(c)/V_0 \approx kc \quad \text{for } c \ll 1/k$$

We therefore plotted $1 - V_{\text{out}}(c)/V_0$ vs. c for $c \ll 1/k$ and again fitted a straight line $mc + b$ with slope m (here expected to equal k) and intercept $b \pm \Delta b$, and using eq. 3 again to find C_{LoD} . Note the different units of m and b between 'off \rightarrow on' and 'on \rightarrow off' evaluation.

Finally, to quantify the quality of a transducer, we define a figure-of-merit (FoM) using k and C_{LoD} . While k and $c_{1/2} = 1/k$ are given by the strength of interaction between dye and analyte only, LoD depends on both, the strength of interaction, and the signal/noise ratio in the transducer. Hence, the ratio given by eq. 6:

$$\text{eq. 6} \quad \text{FoM} = c_{1/2} / C_{\text{LoD}} = 1 / (k * C_{\text{LoD}})$$

is a dimensionless measure of the quality of a transducer. FoM normalises $1/\text{LoD}$ to unit k , *i.e.* separates the contribution of the transducer to lowering LoD from the contribution of k .

3. Results and discussion

a.) Sensor calibration for 'off \rightarrow on' Al^{3+} sensors

Fig. 5 (a and b) show the measured $V_{out}(c)$ for the titration of fresh NaMSA solutions in acidified water as function of $c = [Al^{3+}]$ using different cuvettes. Fig. 5c. is same to fig. 5 (a and b) but with two months old NaMSA solution as described in 2.e. and using PMMA cuvette.

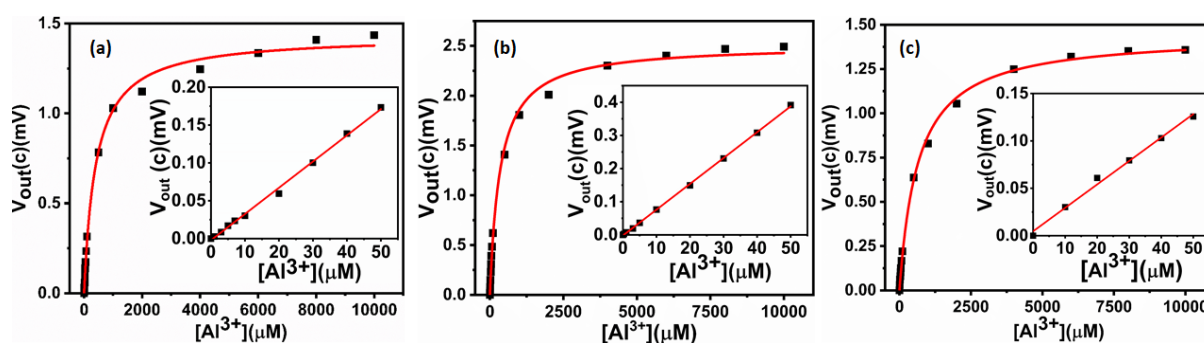


Fig.5. $V_{out}(c)$ as a measure of the fluorescence intensity of NaMSA in (DI-water/ HCl), pH = 5, shown against Al^{3+} concentration from 1 μM to 10 mM, the solid line is the fit to the data using eq. 2 . The insets magnify the linear regime for $[Al^{3+}]$ up to 50 μM . a.) fresh 200 μM NaMSA solution and using the PMMA cuvette, b.) fresh 200 μM NaMSA solution and using the stainless steel cuvette, and c.) two months old NaMSA solution and using the PMMA cuvette.

Fig. 5 clearly confirms that the previously known response of morin (or its derivative, NaMSA) to waterborne Al^{3+} is retained when NaMSA is dissolved in water rather than immobilised in a membrane. The response characteristics are fitted well by the theoretical model, eq. 2, with the best match in the linear regime $c \ll 1/k$, which is the most significant for analysis. The resulting sensor parameters are evaluated as described in the 'Data Analysis' section 2g, and are summarised in table 1.

Table 1

	V_{∞} [mV]	k_c [L/mol]	m [L/mol mV]	b [mV]	Δb [mV]	LoD [μM]
PMMA cuvette 200 μM NaMSA	1.43 ± 0.02	2460 ± 160	3460 ± 60	-0.0021	0.0015	1.3
Steel cuvette	2.51	2800	7790	-0.0018	0.0011	0.4

200 μM NaMSA	± 0.03	± 180	± 50			
PMMA cuvette	$1.45 \pm$	1520	2470	0.0025	0.0032	3.84
old 200 μM NaMSA	0.02	± 80	± 100			

Table1. Parameters obtained from fitting the data in fig. 5 to eq. 2.

As expected, the stability constants, k_c , are similar to each other between the different experimental protocols for fresh NaMSA solution while k_c for the two months old solution is relatively lower. k_c is a property of the interaction of the dye and the analyte in a given medium and should therefore not depend on the details and parameters of experiments undertaken to establish it. We find $k_c \approx 2.5 \times 10^3$ L/mol for the $[\text{MSA}^-:\text{Al}^{3+}]$ complex when both complex partners are dissolved in water. This is about 5 times smaller than k_c for the $[\text{morin}:\text{Al}^{3+}]$ complex for (unmodified) morin in a cellulose membrane at pH in the range 4 to 5 [9]. Further, we find that unlike k_c , the LoD does depend on experimental protocol. Using a reflective stainless steel cuvette leads to a higher V_∞ , as defined in eq. 2, and therefore an improvement in LoD. We therefore recommend the use of reflective cuvettes as a measure to improve LoD with fibre optic instruments, an opportunity inaccessible to conventional fluorimetry. However, even a conventional PMMA cuvette allows the detection of waterborne Al^{3+} with an LoD of $1.3 \mu\text{M}$, below the potability limit of $7.4 \mu\text{M}$ Al^{3+} , despite the relatively small k_c . Even using aged solution and a PMMA cuvette allows detection of waterborne Al^{3+} with an LoD of $3.8 \mu\text{M}$, still below the potability limit of $7.4 \mu\text{M}$ Al^{3+} , despite the relatively small k_c . The LoD reported here is similar to previous work on morin and NaMSA immobilised in a membrane [6, 9, 18]. Here we find value for the FoM, as defined by eq. 6 in section 2g, of $\text{FoM} \approx 300$ for our fibre optic Lock In transducer, which compares very favourably to $\text{FoM} \approx 30$ reported for conventional fluorimetry of Al^{3+} with morin in [9].

b.) Determining Al^{3+} with standard addition method

Three samples, known as 'A, B, C', were analysed in our fluorimeter using the standard addition method. Each sample was tested 4 times. The actual concentrations were not known to the experimenter beforehand, as solutions A, B, C had been prepared

independently by a different worker, who willfully but secretly chose concentrations overlapping the potability limit of Al^{3+} of $7.4 \mu\text{M}$. The resulting standard addition plots are shown below in Fig. 6.

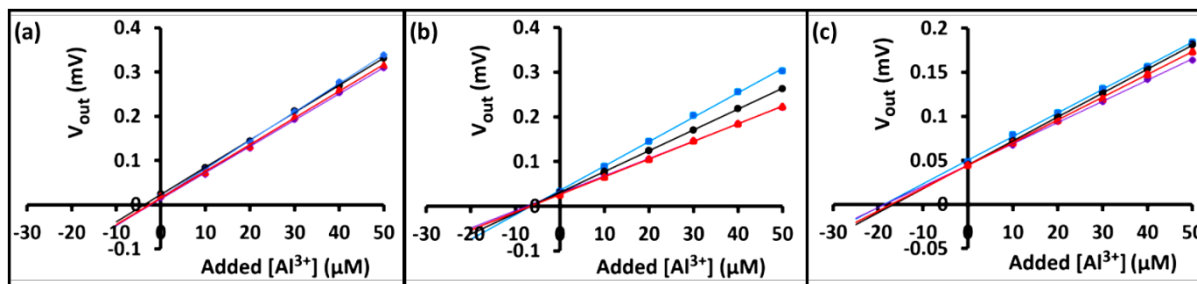


Fig. 6. The standard addition plots, V_{out} vs c_{add} , fitted with straight lines, a.) for sample A b.) for sample B and c.) for sample C. The experiment for each sample was repeated 4 times.

The Al^{3+} concentration in each unknown sample was determined from the standard addition plots as described in 2g. Table 2 summarises all the results compares them to the actual concentrations which were revealed afterward the analysis was completed.

Table 2

Sample A	Measured concentration [μM]	Actual concentration [μM]
1	3.7	3.85
2	2.6	
3	2.2	
4	2.6	
Sample B	Measured concentration [μM]	Actual concentration [μM]
1	6.4	7
2	6.5	
3	6.6	
4	7.4	
Sample C	Measured concentration [μM]	Actual concentration [μM]
1	18.6	17.3
2	16.6	

3	17.0	
4	18.5	

Table 2. The results of the standard addition experiments to determine the Al^{3+} concentration of samples A, B, C, compared to the actual value, which was revealed to the experimenter only in hindsight.

As intended, the standard addition method provides an *in-situ* calibration to account for the small differences between the different fibres, which show as slightly different slopes in the standard addition plots. Nevertheless, the concentrations of samples A, B, and C were determined consistently and repeatably, with an error similar to the LoD of $1.3 \mu\text{M}$, independent of the actual magnitude of $[\text{Al}^{3+}]$. As the potability limit for Al^{3+} is $7.4 \mu\text{M}$, we conclude that dissolved NaMSA as used in our instrument is capable of assessing the potability of water with respect to Al^{3+} .

c.) Sensor calibration for 'on \rightarrow off' F^- sensors

Fig. 7 shows the measured $V_{\text{out}}(c)$ for the titration of solutions of $[\text{MSA}^-:\text{Al}^{3+}]$ complex in acidified water of $\text{pH} = 5$, *i.e.* after 'activation' of NaMSA by Al^{3+} as described in section 2e, as function of $c = [\text{F}^-]$ using different cuvettes. Fig. 7c repeats the experiment shown in fig. 7 (a and b) with a NaMSA solution that was aged for two months.

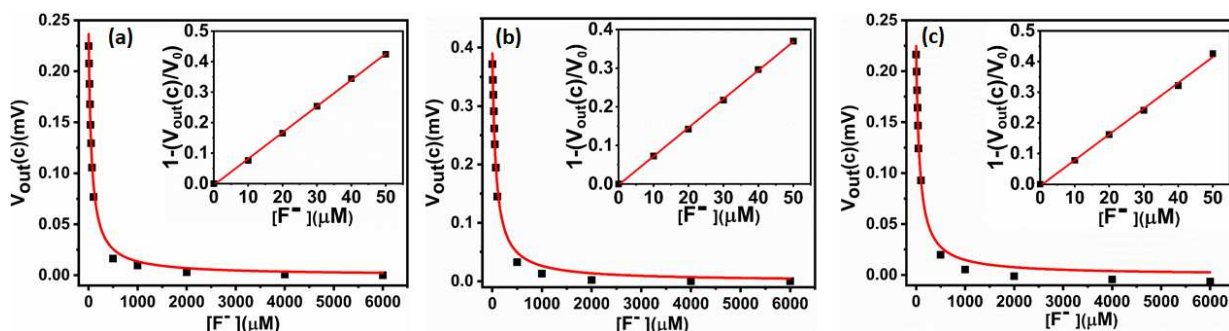


Fig. 7. $V_{\text{out}}(c)$ as a measure of the fluorescence intensity of NaMSA dissolved in (DI water / HCl), $\text{pH} = 5$, and activated with $50 \mu\text{M}$ of Al^{3+} , shown against F^- concentration from $10 \mu\text{M}$ to 6mM . The solid line is a fit to the data using eq. 4. The insets show the linear regime of $1 - (V_{\text{out}}(c)/V_0)$ vs F^- for concentrations up to $50 \mu\text{M}$. The three plots are a.) fresh $200 \mu\text{M}$ NaMSA solution as measured in the PMMA cuvette, b.) fresh $200 \mu\text{M}$ NaMSA solution as

measured in the stainless steel cuvette, and c.) two months old NaMSA as measured in the PMMA cuvette.

Fig. 7 clearly shows that after 'activation' of the NaMSA with Al^{3+} to form the $[\text{MSA}^-:\text{Al}^{3+}]$ complex, this complex then serves as an 'on \rightarrow off' sensor for fluoride ions, F^- . NaMSA was previously considered a dye for the detection of Al^{3+} that can be recovered by adding high concentrations of F^- for de-complexation of $[\text{MSA}^-:\text{Al}^{3+}]$ by F^- [18]. Here we show that NaMSA is in fact a dye suitable for the sensing of either Al^{3+} , or F^- , whichever is of interest. F^- sensitivity can be activated at will simply by prior addition of Al^{3+} , as described in section 2e. Fig. 7c. shows that once NaMSA was activated with Al^{3+} , it remains active for fluoride sensing even after two months of ageing under ambient conditions.

For quantitative analysis, the response characteristics were fitted to eq. 4; LoDs were evaluated from the plots according to eq. 5, as shown as insets to Fig. 7 (a to c), as discussed in section 2g. The results are summarised in table 3.

Table 3

	V_0 [mV]	k_{dc} [L/mol]	m [L/mol]	b	Δb	LoD [μM]
PMMA cuvette 200 μM NaMSA	0.236 ± 0.006	16400 ± 1500	8610 ± 10	-0.0047	0.00322	1.1
Steel cuvette 200 μM NaMSA	0.390 ± 0.010	13800 ± 1290	7410 ± 70	-0.0023	0.00212	0.9
PMMA cuvette aged 200 μM NaMSA	0.225 ± 0.006	14210 ± 1470	8400 ± 197	-0.0084	0.006	2.1

Table 3. Parameters obtained from fitting data in fig. 7(a to c) to eq. 5.

The constant k_{dc} shown in table 3 is the equilibrium constant for the de-complexation of $[\text{MSA}^-:\text{Al}^{3+}]$ complex by F^- . Unsurprisingly, this is different from the k_c previously determined which describes the complexation of MSA^- with Al^{3+} in the absence of F^- . The de-complexation constant is larger, but again it is similar between different experimental

conditions, as expected. Again, the k for aged NaMSA solution activated with Al^{3+} is similar to that obtained from fresh solution. NaMSA solution is stable for at least 2 months. Also, the use of a reflective (stainless steel) cuvette again improves the LoD compared with the PMMA cuvette. LoDs for fresh and aged $[\text{MSA}^-:\text{Al}^{3+}]$ solution are far below potability level for F^- in drinking water, $79 \mu\text{M}$ [4]. As long as an excess of MSA^- is activated by Al^{3+} into the fluoride-sensitive $[\text{MSA}^-:\text{Al}^{3+}]$ complex, it gives a F^- sensor with LoD well below potability over a range of sensitiser concentrations. Note, we have $c_{1/2} = 1/k_{\text{dc}} \approx 70 \mu\text{M}$, hence the highest tested F^- concentration of 6 mM was almost 100 times larger than $c_{1/2}$. It is therefore fair to approximate $V_{\text{out}}(c \rightarrow \infty)$ by $V_{\text{out}}(6\text{mM})$, cf. 2g.

Given the price of the initial morin dye (£72.60 for 10 g) and the yield of 7g NaMSA from 10g morin, each £1 spent on morin dye would provide sufficient solution to fill ~ 4000 cuvettes with $300\mu\text{L}$ of $200 \mu\text{M}$ NaMSA solution. We therefore recommend disposal after single use rather than attempting to re-use dye solutions.

d.) Selectivity for fluoride over chloride

We have tested the selectivity of the $[\text{MSA}^-:\text{Al}^{3+}]$ complex as sensitiser for fluoride over chloride as a potential interferant. In fig. 8 we compare fluoride and chloride titrations under otherwise identical conditions.

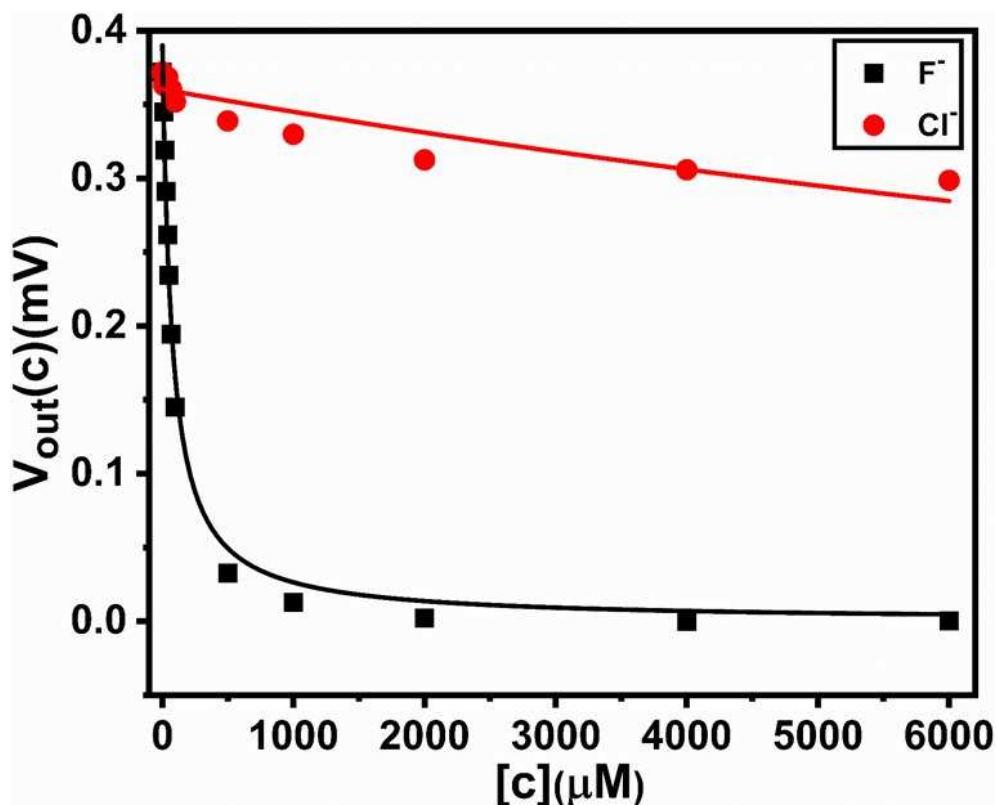


Fig. 8. $V_{out}(c)$ as a measure of the fluorescence of 200 μM NaMSA solution in acidified water activated with 50 μM of Al^{3+} shown against F^- and Cl^- concentration, using the PMMA cuvette. The solid lines represent fits to the data according to eq. 4.

Fig. 8 shows a strong preference of the $[\text{MSA}^-:\text{Al}^{3+}]$ complex to undergo decomplexation with F^- over Cl^- . The (weak) response to Cl^- does not fit to the model presented in eq. 4 well, but when forcibly fitted, nevertheless, we find $k_{dc} = 44 \text{ L/mol}$, hence selectivity is quantified by $\log(k_{dc}(\text{F}^-)/k_{dc}(\text{Cl}^-)) \approx 2.5$. More pragmatically, even large amounts of Cl^- do not reduce the fluorescence intensity to less than 85% of its original value while F^- at potability limit of 79 μM would reduce the fluorescence to less than half its initial value. Interference from Cl^- therefore does not compromise the ability of $[\text{MSA}^-:\text{Al}^{3+}]$ fluorimetry to assess potability with respect to F^- .

e.) The effect of Simultaneous presence of F^- and Al^{3+} on activated NaMSA

In order to investigate the behaviour of our sensitiser to samples which simultaneously contain fluoride *and* aluminium, we first activated a 200 μM NaMSA solution with 50 μM of Al^{3+} . Then we tested the response of this solution by titrating with a mixed (0.75 mM F^- / 0.25 mM Al^{3+}) solution, prepared as described in section 2e. Fig. 9 shows V_{out} first

increasing under the initial activation of NaMSA solution with Al^{3+} , and then its development under titration with the 3:1 mole/mole mixed $\text{F}^- / \text{Al}^{3+}$ solution.

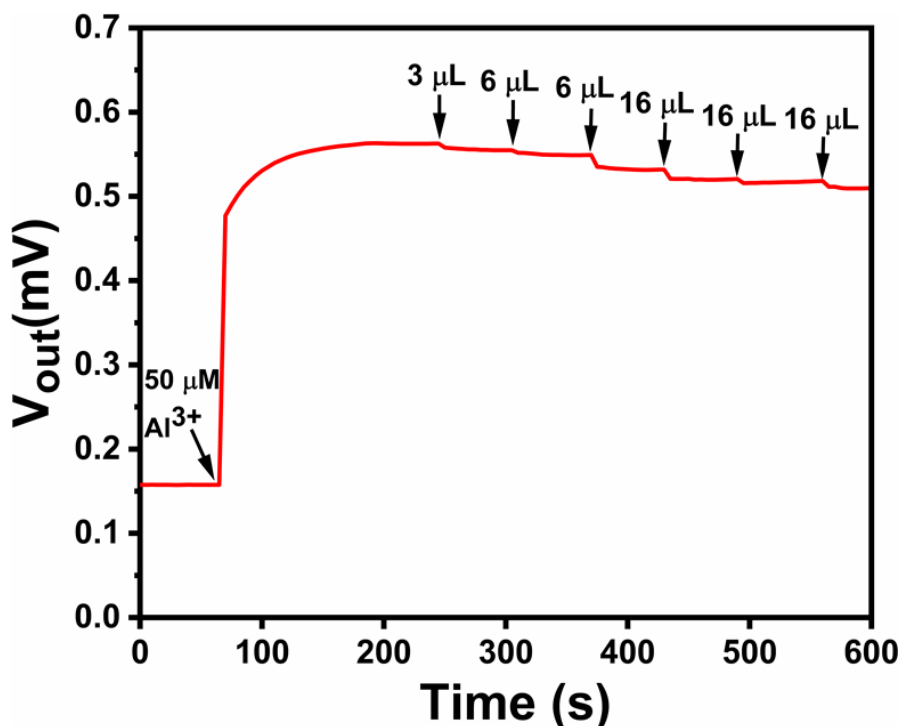


Fig. 9. V_{out} (mV) as a measure of the fluorescence of 200 μM NaMSA solution in acidified water. The first arrow indicates NaMSA activation with 50 μM Al^{3+} , the following arrows indicate the addition of volumes of (0.75 mM / 0.25 mM) mixed $\text{F}^- / \text{Al}^{3+}$ solution.

Fig. 9. shows only a weak response to addition of mixed 0.75 mM $\text{F}^- / 0.25$ mM Al^{3+} solution. Note that the addition of 63 μL of 0.75 mM $\text{F}^- / 0.25$ mM Al^{3+} solution leads to a final concentration of 139.2 μM $\text{F}^- / 46.4$ μM Al^{3+} in the cuvette. Previously, 100 μM F^- reduced the fluorescence of an activated NaMSA solution by 66.3% of its initial value as shown in fig.7 (a) while here, 139.2 μM of F^- added in parallel with 46.4 μM Al^{3+} reduced the fluorescence intensity by only 9.4% of its initial value. On the other hand, the addition of more Al^{3+} would be expected to further increase fluorescence intensity, however this is not observed when the Al^{3+} is added in a 1:3 ratio with fluoride. When fluoride and aluminium are balanced 3:1, they act to cancel each other's effect on the fluorescence intensity of a 200 μM NaMSA solution activated with 50 μM Al^{3+} . Such a solution is therefore not suitable for sensing of either fluoride or aluminium in samples containing both in (3:1) balanced proportions. It may be possible to sense Al^{3+} in mixed $\text{Al}^{3+}/\text{F}^-$ samples when using NaMSA that is at first not activated at all with Al^{3+} , and to sense F^- in mixed $\text{Al}^{3+}/\text{F}^-$ samples when

using NaMSA that is at first ‘fully’ activated with Al^{3+} (in the sense of containing an excess of Al^{3+} over NaMSA), but this was not explored here.

f.) Comparison to prior fluorimetric Al^{3+} and F^- sensors

To assess the quality of our sensors, and in particular our transducer concept, we compare our results for k (k_c and k_{dc}) and LoD to previous reports on fluorimetric Al^{3+} and F^- sensors. A good sensor should have low LoD. However, LoD is controlled by two factors, namely by k that quantifies the ‘strength’ of the analyte / sensitizer interaction (*cf.* the introduction of k in the context of eq. 1 in section 2.g), and the signal-to-noise ratio of the transducer. The transducer’s dimensionless FoM as defined in section 2.g separates the contribution of the transducer from the contribution of k . Table 4 summarises k , LoD, and FoM for a number of fluorimetric sensors for both Al^{3+} and F^- using different sensitizers and transducers, working in different media.

Table 4

No.	Analyte	k [L/mol]	LoD [M]	FoM	Medium	Ref.
1	Al^{3+}	$k_c = 3.3 \times 10^3$	1×10^{-5}	30	MeCN	[27]
2	Al^{3+}	$k_c = 5 \times 10^3$	1×10^{-6}	200	DMF / HEPES	[28]
3	Al^{3+}	$k_c = 3.68 \times 10^4$	1×10^{-6}	27	MeCN / Water	[29]
4	Al^{3+}	$k_c = 1.84 \times 10^4$	2.3×10^{-7}	236	Buffer solution	[30]

5	Al ³⁺	$k_c=1 \times 10^5$	6×10^{-7}	17	DMSO / Water	[31]
6	Al ³⁺	$k_c=9.87 \times 10^4$	3×10^{-8}	337	HEPES buffer	[32]
7	Al ³⁺	$k_c=8.5 \times 10^5$	1.05×10^{-8}	112	DMSO / Water	[33]
8	Al ³⁺	$k_c=5 \times 10^6$	1.35×10^{-9}	148	DI Water	[34]
9	Al ³⁺	$k_c=2.8 \times 10^3$	4×10^{-7}	893	Acidified DI Water	This work
10	F ⁻	$k_{dc}=4.49 \times 10^6$	1×10^{-9}	223	HEPES buffer / DMSO	[35]
11	F ⁻	$k_c=4.69 \times 10^4$	5.8×10^{-7}	37	MeCN	[36]
12	F ⁻	-----	9×10^{-6}	-----	DMSO	[37]
13	F ⁻	$k_c=1 \times 10^4$	2.43×10^{-6}	41	CHCl ₃	[38]
14	F ⁻	$k_{dc}=1.38 \times 10^4$	9×10^{-7}	81	Acidified DI Water	This work

Table 4. Performance parameters of different fluorimetric Al³⁺ and F⁻ sensors. Collated from literature, and tables 1 and 3 in this work. The abbreviations used for the different media refer to MeCN: Acetonitrile, DMSO: Dimethylsulfoxide, DMF: Dimethylformamide, and CHCl₃: Chloroform.

We note that a number of reports sensed Al³⁺ or F⁻ in aprotic polar organic solvents, *e.g.* acetonitrile (MeCN), chloroform, dimethylsulfoxide (DMSO) or dimethylformamide (DMF), or mixtures of such solvents with water, presumably because the sensitizer was not soluble in water. This rather divorces such research from practical applications such as the testing of drinking water. Also, table 4 mostly shows sensitizers for either Al³⁺, or F⁻, but not for both. The use of water-soluble NaMSA works in the aqueous medium without organic additives, and can be adapted to sense both Al³⁺ and F⁻. NaMSA (for Al sensing) and its activated

counterpart (for fluoride sensing) provide LoDs below the potability limits for both Al^{3+} and F^- . Therefore our transducer compares favourably among the sensors working in aqueous medium, since our approach leads to the best FoM for both Al^{3+} and F^- sensing.

4. Conclusions

We extend the use of morin or its derivatives as an Al^{3+} selective 'off \rightarrow on' fluorescent sensitiser when immobilised in a phase transfer membrane to a morin derivative, NaMSA, dissolved in water, avoiding the need for membrane preparation. We develop a fibre optic transducer to demonstrate Al^{3+} detection in drinking water below the potability limit. The dye is very cheap and is stable in solution for several months. We demonstrate it is possible to reliably quantify the concentration of Al^{3+} using the standard addition method. Further, we take advantage of the ability to recover Al^{3+} cation sensors selectively by exposure to fluoride (F^-) anion. Here, we utilise the selective recovery of the dissolved NaMSA- Al^{3+} complex by exposure to F^- to develop a fully 'complementary' sensor for either aluminium cations, or fluoride anions, with LoDs below the potability limit for both of these important water pollutants. Dissolved NaMSA works as 'off-to-on' sensor for Al^{3+} cations. In order to become sensitive to F^- , the NaMSA must first be 'activated' by deliberately adding Al^{3+} to form the $[\text{MSA}^-:\text{Al}^{3+}]$ complex, which then acts as sensitiser for 'on \rightarrow off' fluorescent sensing of the F^- anion. In complementary sensing, the conventional distinction between 'sensing' and 'recovery' is lifted. We propose that other ion selective dyes with known recovery agents could be used in a similar manner to produce a wide range of low cost complementary ion sensors. We further recommend our lock-in fibre optic transducer concept as an alternative to conventional spectrofluorimeters, which can demonstrate a higher figure- of- merit at lower footprint.

Acknowledgements Alhulw H Alshammari thanks the Cultural Attaché of Saudi Arabia to the UK and Aljouf University for the award of a PhD scholarship. Zahrah Alqahtani thanks the Cultural Attaché of Saudi Arabia to the UK and Taif University, Saudi Arabia, for providing her with fellowships for her Ph.D. studies. F B Mohd Suah would like to thank Universitiy Sains Malaysia for providing financial assistance through USM short term grant (304 / PKIMIA / 6315197).

References

- [1] Liu, Y., Bi, A., Gao, T., Cao, X., Gao, F., Rong, P., Wang, W. and Zeng, W., 2019. A novel self-assembled nanoprobe for the detection of aluminum ions in real water samples and living cells. *Talanta*, 194, pp.38-45.
- [2] Perl, D.P. and Good, P.F., 1991. Aluminum, Alzheimer's disease, and the olfactory system. *Annals of the New York Academy of Sciences*, 640(1), pp.8-13.
- [3] Meng, Q., Liu, H., Sen, C., Cao, C. and Ren, J., 2012. A novel molecular probe sensing polynuclear hydrolyzed aluminum by chelation-enhanced fluorescence. *Talanta*, 99, pp.464-470.
- [4] <https://www.lenntech.com/applications/drinking/standards/eu-s-drinking-water-standards.htm>. (Accessed 20 December 2019).
- [5] Ahmed, M.J., Hoque, M.R., Khan, A.S.H. and Bhattacharjee, S.C., 2010. A Simple Spectrophotometric Method for the Determination of Aluminum in Some Real, Environmental, Biological, Soil and Pharmaceutical Samples Using 2-Hydroxynaphthaldehydebenzoylhydrazone. *Eurasian Journal of Analytical Chemistry*, 5(1), pp.1-15.
- [6] Suah, F.B.M. and Ahmad, M., 2017. Preparation and characterization of polymer inclusion membrane based optode for determination of Al³⁺ ion. *Analytica Chimica Acta*, 951, pp.133-139.

- [7] Aziz, A.A.A., Mohamed, R.G., Elantabli, F.M. and El-Medani, S.M., 2016. A Novel Fluorimetric Bulk Optode Membrane Based on NOS Tridentate Schiff Base for Selective Optical Sensing of Al^{3+} Ions. *Journal of Fluorescence*, 26(6), pp.1927-1938.
- [8] Gupta, V.K., Jain, A.K. and Maheshwari, G., 2007. Aluminum (III) selective potentiometric sensor based on morin in poly (vinyl chloride) matrix. *Talanta*, 72(4), pp.1469-1473.
- [9] Saari, L.A. and Seitz, W.R., 1983. Immobilized morin as fluorescence sensor for determination of aluminum (III). *Analytical Chemistry*, 55(4), pp.667-670.
- [10] Nizar, S.A., Satar, N.S.A., Amar, S.A.S., Abdullah, F.H., Mehamod, F.S. and Suah, F.B.M., 2019. Fluorescence enhancement of Al^{3+} -sodium morin-5-sulfonate complex by imidazolium ionic liquid and its application in determination of Al^{3+} ions in an aqueous solution. *Jurnal Teknologi*, 81(2), pp.175-180.
- [11] Kopacz M., 2003, Quercetin- and Morinsulfonates as Analytical Reagents. *Journal of Analytical Chemistry*, 58(3), pp. 258-262.
- [12] Saleh, S.M., Ali, R. and Ali, I.A., 2017. A novel, highly sensitive, selective, reversible and turn-on chemi-sensor based on Schiff base for rapid detection of Cu (II). *Spectrochimica Acta Part A: Molecular and Biomolecular Spectroscopy*, 183, pp.225-231.
- [13] Niu, C.G., Guan, A.L., Zeng, G.M., Liu, Y.G. and Li, Z.W., 2006. Fluorescence water sensor based on covalent immobilization of chalcone derivative. *Analytica Chimica Acta*, 577(2), pp.264-270.
- [14] Çağlar, Y., Saka, E.T., Alp, H., Kantekin, H., Ocak, Ü. and Ocak, M., 2016. A simple Spectrofluorimetric method based on quenching of a nickel (II)-Phthalocyanine complex to determine iron (III). *Journal of Fluorescence*, 26(4), pp.1381-1389.
- [15] Tang, Y., Ding, Y., Wu, T., Lv, L. and Yan, Z., 2016. A turn-on fluorescent probe for Hg^{2+} detection by using gold nanoparticle-based hybrid microgels. *Sensors and Actuators B: Chemical*, 228, pp.767-773.
- [16] Panchenko, P.A., Fedorov, Y.V. and Fedorova, O.A., 2018. Selective fluorometric sensing of Hg^{2+} in aqueous solution by the inhibition of PET from dithia-15-crown-5 ether receptor

conjugated to 4-amino-1, 8-naphthalimide fluorophore. *Journal of Photochemistry and Photobiology A: Chemistry*, 364, pp.124-129.

[17] Ghosh, S., Khan, M.A., Ganguly, A., Al Masum, A., Alam, M.A. and Guchhait, N., 2018. Binding mode dependent signaling for the detection of Cu^{2+} : An experimental and theoretical approach with practical applications. *Spectrochimica Acta Part A: Molecular and Biomolecular Spectroscopy*, 190, pp.471-477.

[18] Suah, F.B.M., Ahmad, M. and Heng, L.Y., 2014. Highly sensitive fluorescence optode for aluminium (III) based on non-plasticized polymer inclusion membrane. *Sensors and Actuators B: Chemical*, 201, pp.490-495.

[19] Alshammari, A.H., Kirwa, A., Dunbar, A. and Grell, M., 2019. Adaptive and sensitive fibre-optic fluorimetric transducer for air-and water-borne analytes. *Talanta*, 199, pp.40-45.

[20] Bruce, G.R. and Gill, P.S., 1999. Estimates of precision in a standard additions analysis. *Journal of Chemical Education*, 76(6), p.805.

[21] Ke, B., Chen, W., Ni, N., Cheng, Y., Dai, C., Dinh, H. and Wang, B., 2013. A fluorescent probe for rapid aqueous fluoride detection and cell imaging. *Chemical Communications*, 49(25), pp.2494-2496.

[22] Xiong, L., Feng, J., Hu, R., Wang, S., Li, S., Li, Y. and Yang, G., 2013. Sensing in 15 s for aqueous fluoride anion by water-insoluble fluorescent probe incorporating hydrogel. *Analytical chemistry*, 85(8), pp.4113-4119.

[23] Tuwei, K.A., Williams, N.H. and Grell, M., 2016. Fibre optic absorbance meter with low limit of detection for waterborne cations. *Sensors and Actuators B: Chemical*, 237, pp.1102-1107.

[24] Tuwei, A.K., Williams, N.H., Mulla, M.Y., Di Natale, C., Paolesse, R. and Grell, M., 2017. 'Rough guide' evanescent wave optrode for colorimetric metalloporphyrine sensors. *Talanta*, 164, pp.228-232.

[25] Ma, T., Zhao, X., Matsuo, Y., Song, J., Zhao, R., Faheem, M., Chen, M., Zhang, Y., Tian, Y. and Zhu, G., 2019. Fluorescein-based fluorescent porous aromatic framework for Fe^{3+} detection with high sensitivity. *Journal of Materials Chemistry C*, 7(8), pp.2327-2332.

- [26] Bruce, G.R. and Gill, P.S., 1999. Estimates of precision in a standard additions analysis. *Journal of Chemical Education*, 76(6), p.805.
- [27] Jang, Y.K., Nam, U.C., Kwon, H.L., Hwang, I.H. and Kim, C., 2013. A selective colorimetric and fluorescent chemosensor based-on naphthol for detection of Al^{3+} and Cu^{2+} . *Dyes and Pigments*, 99(1), pp.6-13.
- [28] Kim, K.B., You, D.M., Jeon, J.H., Yeon, Y.H., Kim, J.H. and Kim, C., 2014. A fluorescent and colorimetric chemosensor for selective detection of aluminum in aqueous solution. *Tetrahedron Letters*, 55(7), pp.1347-1352.
- [29] Singh, V.P., Tiwari, K., Mishra, M., Srivastava, N. and Saha, S., 2013. 5-[(2-Hydroxynaphthalen-1-yl) methylene] amino] pyrimidine-2, 4 (1H, 3H)-dione as Al^{3+} selective colorimetric and fluorescent chemosensor. *Sensors and Actuators B: Chemical*, 182, pp.546-554.
- [30] In, B., Hwang, G.W. and Lee, K.H., 2016. Highly sensitive and selective detection of Al (III) ions in aqueous buffered solution with fluorescent peptide-based sensor. *Bioorganic & medicinal chemistry letters*, 26(18), pp.4477-4482.
- [31] Kejík, Z., Kaplánek, R., Havlík, M., Bříza, T., Vavřinová, D., Dolenský, B., Martásek, P. and Král, V., 2016. Aluminium (III) sensing by pyridoxal hydrazone utilising the chelation enhanced fluorescence effect. *Journal of Luminescence*, 180, pp.269-277.
- [32] Xie, J.Y., Li, C.Y., Li, Y.F., Fu, Y.J., Nie, S.X. and Tan, H.Y., 2017. A near-infrared chemosensor for determination of trivalent aluminum ions in living cells and tissues. *Dyes and Pigments*, 136, pp.817-824.
- [33] Sarkar, D., Ghosh, P., Gharami, S., Mondal, T.K. and Murmu, N., 2017. A novel coumarin based molecular switch for the sequential detection of Al^{3+} and F^- : application in lung cancer live cell imaging and construction of logic gate. *Sensors and Actuators B: Chemical*, 242, pp.338-346.
- [34] Dwivedi, R., Singh, D.P., Chauhan, B.S., Srikrishna, S., Panday, A.K., Choudhury, L.H. and Singh, V.P., 2018. Intracellular application and logic gate behavior of a 'turn off-on-off' type probe for selective detection of Al^{3+} and F^- ions in pure aqueous medium. *Sensors and Actuators B: Chemical*, 258, pp.881-894.

- [35] Selvaraj, M., Rajalakshmi, K., Nam, Y.S., Lee, Y., Song, J.W., Lee, H.J. and Lee, K.B., 2019. On-off-on relay fluorescence recognition of ferric and fluoride ions based on indicator displacement in living cells. *Analytica chimica acta*, 1066, pp.112-120.
- [36] Bhattacharyya, B., Kundu, A., Guchhait, N. and Dhara, K., 2017. Anthraimidazoledione Based Reversible and Reusable Selective Chemosensors for Fluoride Ion: Naked-Eye, Colorimetric and Fluorescence "ON-OFF". *Journal of fluorescence*, 27(3), pp.1041-1049.
- [37] Yu, M., Xu, J., Peng, C., Li, Z., Liu, C. and Wei, L., 2016. A novel colorimetric and fluorescent probe for detecting fluoride anions: from water and toothpaste samples. *Tetrahedron*, 72(2), pp.273-278.
- [38] Thongkum, D. and Tuntulani, T., 2011. Fluoride-induced intermolecular excimer formation of bispyrenyl thioureas linked by polyethylene glycol chains. *Tetrahedron*, 67(42), pp.8102-8109.